Global Visual Motion Sensitivity: Associations with Parietal Area and Children's Mathematical Cognition

Oliver Braddick[1], Janette Atkinson[2], Erik Newman[3], Natacha Akshoomoff[3],
Joshua M. Kuperman[3], Hauke Bartsch[3], Chi-Hua Chen[3], Anders M. Dale[3],
and Terry L. Jernigan[3]

Abstract

■ Sensitivity to global visual motion has been proposed as a signature of brain development, related to the dorsal rather than ventral cortical stream. Thresholds for global motion have been found to be elevated more than for global static form in many developmental disorders, leading to the idea of "dorsal stream vulnerability." Here we explore the association of global motion thresholds with individual differences in children's brain development, in a group of typically developing 5- to 12-year-olds. Good performance was associated with a relative increase in parietal lobe surface area, most strongly around the intraparietal sulcus and decrease in occipital area. In line with the involvement of intraparietal sulcus, areas in visuospatial and numerical cognition, we also found that global motion perfor-

mance was correlated with tests of visuomotor integration and numerical skills. Individual differences in global form detection showed none of these anatomical or cognitive correlations. This suggests that the correlations with motion sensitivity are unlikely to reflect general perceptual or attentional abilities required for both form and motion. We conclude that individual developmental variations in global motion processing are not linked to greater area in the extrastriate visual areas, which initially process such motion, but in the parietal systems that make decisions based on this information. The overlap with visuospatial and numerical abilities may indicate the anatomical substrate of the "dorsal stream vulnerability" proposed as characterizing neurodevelopmental disorders. ■

INTRODUCTION

The ability to detect coherent global motion is a sensitive signature of typical and atypical brain development. Performance, which is measurable in infancy (Biagi, Crespi, Tosetti, & Morrone, 2015; Wattam-Bell et al., 2010; Wattam-Bell, 1994), shows a strong developmental trend in middle childhood (Atkinson & Braddick, 2005; Gunn et al., 2002), developing relatively slowly compared with the analogous measure for global static form. This study examines children's individual variation in this ability and its relation to brain structure and other cognitive functions.

Global motion sensitivity is specifically impaired, compared with global static form, in a range of genetic and acquired developmental disorders including Williams syndrome, autism, fragile-X syndrome, and children with very preterm birth (Braddick & Atkinson, 2011; Braddick, Atkinson, & Wattam-Bell, 2003). This differential impairment has led us to propose the hypothesis of "dorsal stream vulnerability" (Braddick et al., 2003). In addition, children with disorders that show a global motion deficit compared with form coherence thresholds typically also show problems in visuospatial, attentional, and visuomotor

abilities associated with networks in the dorsal stream of cortical processing (Atkinson & Braddick, 2007, 2011, 2012; Kravitz, Saleem, Baker, & Mishkin, 2011).

The ability to detect global organization in visual patterns reflects processing beyond the initial cortical visual areas, because it requires receptive fields large enough to integrate information from many local elements. fMRI and non-human primate studies show a network of extrastriate brain areas with integrative functions including sensitivity to coherent global motion; these include the extrastriate area V5 (MT) (Albright & Stoner, 1995; Britten, Shadlen, Newsome, & Movshon, 1992; Newsome & Paré, 1988) and other areas in the dorsal cortical stream, such as MST, V3A, V6, and the intraparietal sulcus (IPS) (Helfrich, Becker, & Haarmeier, 2013; Pitzalis et al., 2010; Orban et al., 2003; Braddick, O'Brien, Wattam-Bell, Atkinson, & Turner, 2001; Sunaert, Van Hecke, Marchal, & Orban, 1999). The dorsal stream projects to parietal cortex (Milner & Goodale, 1995; Mishkin, Ungerleider, & Macko, 1983) and on to multiple, more anterior areas concerned with spatial, visuomotor, and attentional function (Kravitz et al., 2011). The areas activated by global motion coherence are independent of those activated by static global form (Braddick, O'Brien, Wattam-Bell, Atkinson, & Turner, 2000), which in macaque begin with extrastriate area V4 (Gallant, Braun, & Van Essen, 1993) and form part of the ventral cortical stream.

---

[1]University of Oxford, [2]University College London, [3]University of California San Diego

However, it is not known whether the relatively poor sensitivity to global motion found in developmental disorders such as hemiplegia, autism, Williams syndrome, and dyslexia relates to early extrastriate areas such as V5(MT) or the cortical networks to which these extrastriate areas project. Nor do we know how far global motion deficits are directly associated with the deficits in visuospatial, visuomotor, and attentional function, which characterize these disorders, or whether these are functionally independent results of pathological processes.

We aimed to throw light on these questions through measurements of typical development in a sample of children, aged 5–12 years, who received structural neuroimaging. We have examined correlations of children's individual global motion and form sensitivity with structural variations in different brain areas, in particular local cortical area, which has been found to be a robust and powerful measure of cortical development (Lyall et al., 2015; Raznahan et al., 2011) and has been successfully related to behavioral functions (Newman et al., 2016; Fjell, Westlye, et al., 2015; Fjell et al., 2012). Specifically, we test the hypothesis that sensitivity to global motion is related to the surface area of parietal and occipital cortex and that this pattern differs from sensitivity to global form.

We also examine how global motion and form sensitivity correlate with normal variations in tests of cognitive function and achievement. In particular, we examine the relationship with functions believed to be subserved by dorsal stream and parietal areas. Evidence from functional neuroimaging, effects of transcranial stimulation, and lesion effects implicates parietal cortical areas—particularly around the IPS—in a range of calculation tasks and numerosity judgments (e.g., Butterworth & Walsh, 2011; Holloway & Ansari, 2010; Menon, 2010; Nieder & Dehaene, 2009). A direct relationship between motion sensitivity and numerical representations is further suggested in the finding in macaques that the majority of IPS neurons that are sensitive to numerosity are also sensitive to optic flow patterns (Tudusciuc & Nieder, 2007). We have therefore specifically examined the relations between children's global motion performance and tests of calculation abilities, numerical judgments, and visuomotor skills, detailed in the Methods section. To test how specific these relationships were to mathematical and visuospatial performance, reading scores were also analyzed.

METHODS

Participants

The participants were drawn from a sample of children (N = 154) in the PING (Pediatric Imaging, Neurocognition & Genetics) and PLING (Pediatric Longitudinal Imaging, Neurocognition & Genetics) studies (Jernigan, Brown, Hagler, et al., 2016; Akshoomoff et al., 2014; Brown et al., 2012; Fjell et al., 2012; see ping.chd.ucsd.edu), assessed in the age range 5–12 years. They received, in addition to measurements of global form and motion sensitivity, measurements of gray and white matter from structural MRI and an extensive battery of cognitive tests, including tests of mathematical cognition and achievement. PING is a multicenter study, but the global form and global motion measures were included in the study protocol only at the University of California, San Diego, and all children whose data are presented here were studied at that center. The human research protections program and institutional review board at University of California, San Diego, approved all experimental and consenting procedures. Written parental informed consent was obtained for all participants and child assent for those 7 years and older. Participants were screened for history of major developmental, psychiatric, or neurological disorders, brain injury, or other medical conditions that affect development. Only participants aged between 5:0 and 12:11 years, who completed two measurements of both global motion and global form sensitivity, with cortical and subcortical segmentations of neuroimaging data that passed quality check, were included.

The total sample included 154 children (78 boys, 76 girls), mean age = 7.75 years (SD = 1.91 years); the distribution between 1-year age bands is given in Table 1.

Global Form and Motion Testing

Sensitivity to global motion and form was determined by the threshold for detecting global structure as a percentage of coherently organized elements embedded among random noise elements. The test followed a similar procedure to that of Gunn et al. (2002) but with concentric stimulus displays (Atkinson & Braddick, 2005), which are designed to make the form and motion tasks as comparable as possible. Participants viewed a laptop computer screen and had to report whether a circular region, containing concentrically organized short arcs or trajectories of moving dots, appeared on the left or right of center in a background of randomly oriented elements.

The display area was 25 × 18 deg arc at the viewing distance of 50 cm. The global motion display contains 3000 dots size 11 min arc diameter, moving at 4.1 deg/sec. Each dot has a lifetime of eight frames (133 msec), after which it disappears from the screen. Within a circular target region diameter 9.5 deg arc, centered 6.3 deg left or right of screen center, coherent dots move in concentric

Table 1. Age Distribution of Participating Children

Age range (years:months)	5:0–5:11	6:0–6:11	7:0–7:11	8:0–8:11	9:0–9:11	10:0–11:11
n	38	26	23	33	19	21

circular paths. The percentage of dots sharing this coherent motion varies from trial to trial as described below. The remaining dots within this region and all the dots elsewhere on the screen move in randomly oriented arcs with the same distribution of curvature as the population of coherently moving dot trajectories.

The global form display contains 3000 stationary arc segments, 8 min arc width × 42 min arc length. Within a circular target region with the same parameters as in the global motion display, the coherent arcs are oriented to be concentric. The percentage of arcs sharing this coherent alignment varies according to the same adaptive procedure as for motion. The remaining arcs within this region and all the arcs elsewhere on the screen are randomly oriented arcs with the same distribution of curvature as the coherently oriented arcs.

Participants completed four test runs, alternating runs with the global form and global motion display, with the starting test randomized across participants. On each trial, the structured target region was presented randomly on the left or right of center, and the child was asked to point to the side that contained the circular pattern, or for older children to press the corresponding arrow key on the keyboard. Each run began with coherence fixed at 100%, and these trials were continued until the tester was satisfied that the child understood the task. In the following test phase, the coherence level of the target region was varied according to the PSI adaptive procedure (Kontsevich & Tyler, 1999), which uses a Bayesian approach to place each trial at the point where it will give the most information about the two-dimensional posterior probability distribution of the threshold and slope of the psychometric function. The estimated threshold is the mean threshold from this distribution, after the completion of 30 trials. Because the adaptive procedure leads to difficult decisions as stimuli are delivered increasingly close to the individual's threshold, participants' motivation was maintained by delivering an easily visible stimulus (100% coherence) on every sixth trial.

Cognitive and Achievement Tests

An extensive battery of cognitive and achievement tests is incorporated in the PING and PLING studies. In the present report, we restrict analysis to those relevant to our hypotheses as discussed in the Introduction. These comprised children's abilities for calculation, assessed by the Woodcock–Johnson tests (Woodcock, McGrew, & Mather, 2001), in which the Calculation Test measures the ability to perform simple written calculations and the Applied Problems test measures skill in analyzing and solving practical numerical word problems; numerical judgments assessed by the Panamath test (Halberda & Feigenson, 2008; www.panamath.org/index.php); and visuomotor performance from the Test of Visuomotor Integration (VMI; Beery, 1989). The Panamath test presents participants with arrays of yellow and blue spots in a

1200-msec exposure (too brief for counting) and requires them to report whether there are more yellow or more blue spots. The ratio varies from trial to trial. For the current study, performance was measured as the overall percentage of correct trials in blocks over four ratios (1:1.2, 1:1.5, 1:2, 1:3). Although the Weber fraction for numerosity judgments may provide the most quantitative measure of performance of the "approximate number system" (Halberda & Feigenson, 2008), experience with this test indicated that, as some children were above the threshold and others were below it at all stimulus levels, the Weber fraction could not be reliably interpolated. Inglis and Gilmore (2014) present theoretical and empirical arguments on this issue, concluding that overall percent correct is the most robust way of indexing the acuity of an individual's approximate number system, and we have followed this recommendation.

To test how far these relationships were specific to mathematical and visuospatial performance, scores of single word reading from the NIH Toolbox Oral Reading Recognition Test (Akshoomoff et al., 2014; Gershon et al., 2010) were also analyzed.

Data were not available for all these cognitive measures on every participant; numbers available for each test are indicated in the rightmost column of Table 5.

Neuroimaging and Analysis: MRI Scanning Protocol

The neuroimaging protocol was as described in Jernigan, Brown, Hagler, et al. (2016). A standardized multiple-modality high-resolution structural MRI protocol was implemented involving 3-D T1-weighted volumes and a set of diffusion-weighted scans, on a GE 3T Signa HDx scanner and a 3T Discovery 750x scanner (GE Healthcare, Little Chalfont, United Kingdom) using eight-channel-phased array head coils. The protocol included a conventional three-plane localizer, a sagittal 3-D inversion recovery spoiled gradient-echo T1-weighted volume optimized for maximum gray/white matter contrast (echo time = 3.5 msec, repetition time = 8.1 msec, inversion time = 640 msec, flip angle = 8°, receiver bandwidth = ±31.25 kHz, field of view = 24 cm, frequency = 256, phase = 192, slice thickness = 1.2 mm), and two axial 2-D diffusion tensor imaging pepolar scans (30-directions b value = 1,000, echo time = 83 msec, repetition time = 13,600 msec, frequency = 96, phase = 96, slice thickness = 2.5 mm).

Image postprocessing and analysis were performed using a fully automated set of tools available in the Free-surfer software suite (surfer.nmr.mgh.harvard.edu/; Fischl, Salat, et al., 2004; Fischl, van der Kouwe, et al., 2004; Dale, Fischl, & Sereno, 1999). Continuous maps of cortical surface area were obtained by computing the area of each triangle of a standardized tessellation mapped to each subject's native space using a spherical atlas registration procedure (Fischl, Sereno, & Dale, 1999). This mapping provides point-by-point estimates of the relative areal expansion or compression of each
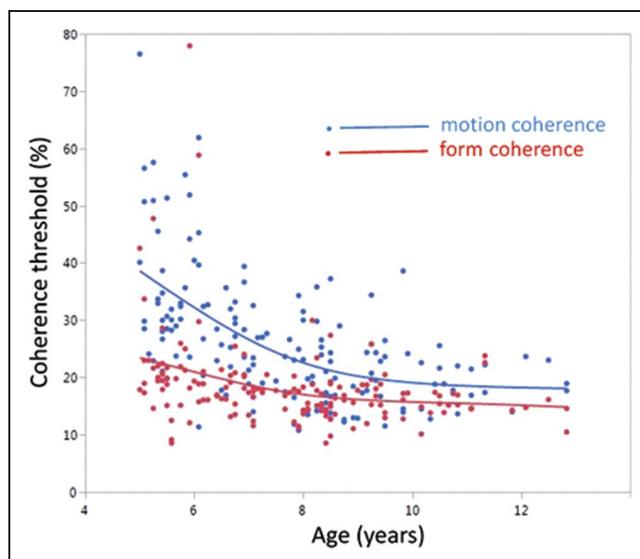
Figure 1. Individual children's coherence thresholds for global motion (blue) and global form (red), plotted as a function of age. Each point is the mean of two measurements. The lines are smoothed fits to the data points. $N = 154$.

location in atlas space, yielding a pointwise measure of cortical surface area.

Analyses of the Relation of Behavioral Measures to Vertex-wise Areal Expansion

The initial analysis related motion and form coherence thresholds to the areas of four major lobes (occipital, parietal, temporal, and frontal) defined from a novel, genetically informed, cortical parcellation scheme, derived from results obtained using a fuzzy clustering method to analyze the matrix of genetic correlations among vertex-wise estimates of cortical surface expansion in a sample of monozygotic and dizygotic twins (Chen et al., 2012). Parcels within each lobe, combining the two hemispheres, were combined to define four lobar areas for each participant. Models were computed for the area of each lobe, with age, age-squared, sex, scanner, total cor-

tical area, coherence threshold, and interaction of coherence threshold with age as predictors.

To explore in more detail the topography of cortical area expansion associated with test results, we used the PING Data Exploration Portal (Bartsch, Thompson, Jernigan, & Dale, 2014), a Web-based tool for modeling PING data to estimate the vertex-wise anatomical variability of association with global motion and form sensitivity for relative cortical surface area. Age, age-squared, sex, scanner, total area, and the interaction of global motion sensitivity with age were taken out as covariates, and the significance level of the association mapped over the cortical surface.

RESULTS

Motion and Form Coherence Thresholds as a Function of Age

Figure 1 plots thresholds for global form and global motion, as a function of age at test, with quadratic fits to the age functions. Both thresholds show improvement over the age range, in line with previously published data (Atkinson & Braddick, 2005; Gunn et al., 2002). ANOVA confirms a significant linear, $F(1, 150) = 66.9, p < .0001$, and quadratic, $F(1, 150) = 14.2, p < .0001$, variation with age and that motion thresholds are numerically higher than form thresholds, $F(1, 150) = 75.9, p < .0001$. More importantly, task (motion vs. form) shows a significant interaction with age, $F(1, 150) = 40.1, p < .0001$, and age-squared, $F(1, 150) = 9.48, p < .0025$, reflecting the steeper improvement with age seen for global motion, especially among the younger children. Global motion thresholds also show greater interindividual variability than form thresholds, as tested by calculating the absolute value of residuals against the quadratic function of age for each measure and comparing these values as matched-pairs between form and motion ($t = 2.68, p < .0001$).

Relationships to Local Cortical Area Expansion

First, regression models for global form and motion thresholds were tested with the bilateral area of each of

Table 2. Results of Regression Models Predicting Global Motion and Form Thresholds from Bilateral Cortical Surface Areas of Each of the Four Cerebral Lobes

Term	Global Motion, t	Global Motion, p	Global Form, t	Global Form, p
Occipital area	**2.15**	**.033***	0.30	.76
Parietal area	**−2.08**	**.040***	0.43	.67
Temporal area	0.33	.58	0.01	.99
Frontal area	−0.55	.74	−1.05	.29

The full models included as nuisance variables age, age-squared, sex, MRI scanner, and interactions. Variables predicting high sensitivity show a negative effect because this corresponds to low threshold. Fuller results of the regression models are presented in Appendix A (Table A1).

Boldface indicates significant results.

*$p < .05$
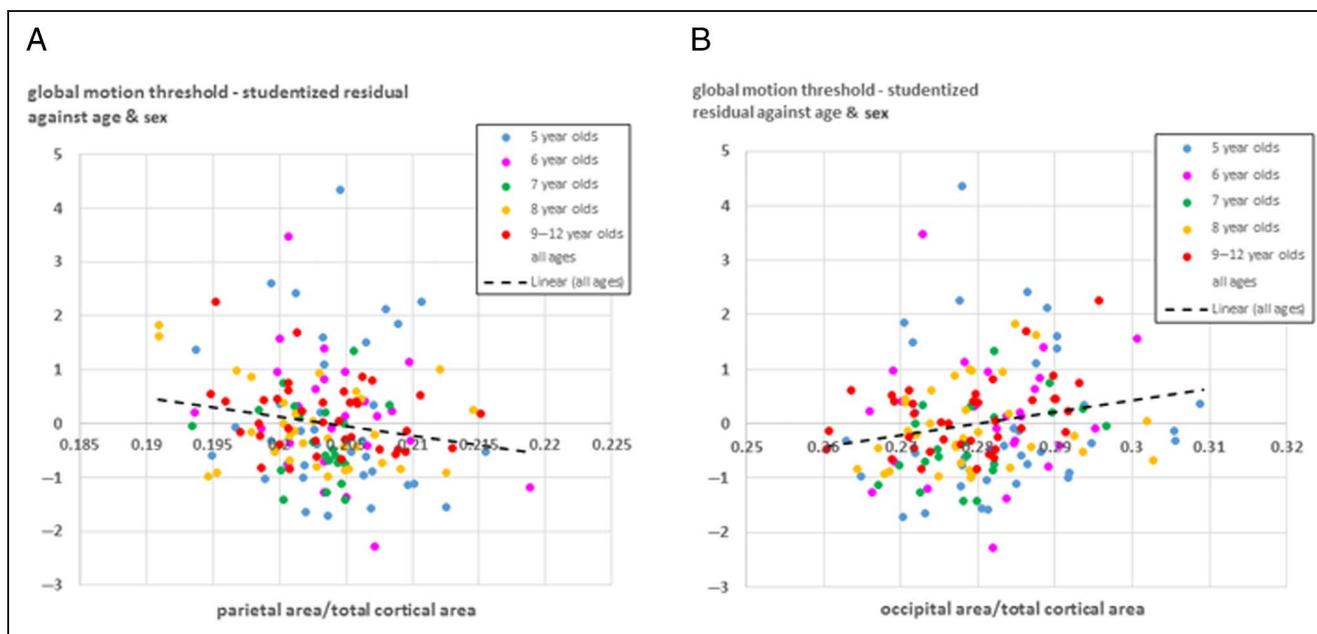
Figure 2. The relationship between children's motion coherence thresholds and the areas of parietal and occipital lobes. *x* axis: Studentized residuals of motion coherence threshold after controlling for age and sex. *y* axis: The proportion of total cortical surface area occupied by the parietal lobe (A, left) and occipital lobe (B, right). Colors of points indicate age groups (see key). The regression line (black dashed) is derived from the whole sample.

the four lobes as simultaneous predictors. Age, age-squared, sex, and MRI scanner were included as "nuisance" covariates. Results for the variables of interest are shown in Table 2. Higher global motion sensitivity was significantly associated with relatively larger area of the parietal lobe, and relatively smaller area of the occipital lobe. Figure 2 shows the studentized residual of motion coherence threshold after controlling for age and sex, plotted against the proportion of total area occupied by the parietal lobe (Figure 2A) and occipital lobe (Figure 2B). Global form performance showed no evidence of association with any of the four areas measured.

To examine further how far the associations with cortical area reflect specific patterns of arealization, as distinct from generally increased cortical area, we tested further models in which the surface areas of occipital and parietal lobes were used separately as predictors of global motion thresholds, with total cortical area (and the other "nuisance factors"—see table legend) included as covariates (Table 3). The results confirm that relatively larger parietal area and relatively smaller occipital area are associated with higher global motion sensitivity. Total cortical area is an additional predictor of high motion thresholds (low sensitivity) in the analysis using parietal area and shows a nonsignificant association with low motion thresholds (high sensitivity) in the analysis using occipital area. This pattern of results suggests that the additional contribution of total area simply reflects the opposite influences of occipital area in the former case and parietal area in the latter.

To examine whether these results might reflect variations in overall brain maturation, reflected in the relation

Table 3. Results of Regression Models Testing Separately the Prediction of Global Motion Thresholds from Bilateral Parietal Area and Bilateral Occipital Area

| | Model for Global Motion Threshold | | | |
| | Bilateral Lobe Area | | Total Cortical Area | |
Predictor	t Ratio	p	t Ratio	p
Parietal area	**−2.36**	**.019***	1.58	.12
Occipital area	**2.42**	**.017***	**−3.21**	**.0016***

The full model included as nuisance variables age, age-squared, sex, MRI scanner, and interactions. Variables predicting high sensitivity show as a negative effect, because this corresponds to low threshold. Fuller results of the regression models are presented in Appendix A (Table A2).

Boldface indicates significant results.

*p < .05.

Table 4. Parietal/Occipital Area Ratio Is Independent of Age: Results of Regression Model Testing Prediction of This Ratio from Age and Age-squared

| Prediction | Parietal/Occipital Area Ratio from Age | |
Term	t Ratio	Prob > |t|
Intercept	48.68	<0.0001
Age	1.18	0.24
Age-squared	0.14	0.89

Fuller results of the regression model are presented in Appendix A (Table A3).
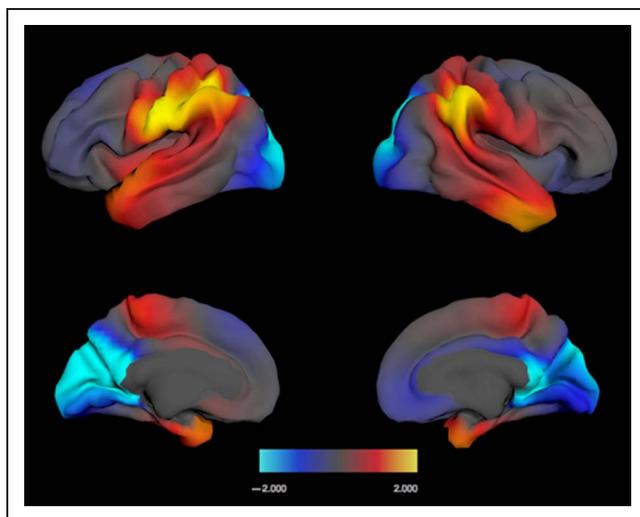
Figure 3. Maps showing the vertex-wise variability of association between local cortical area and individual sensitivity to global motion coherence. Top row = lateral view; bottom row = medial view. left = left hemisphere; right = right hemisphere. The models used to compute these maps controlled for scanner, age, sex, and total surface area. The color scale shows the significance of positive and negative associations in a range up to $p = .01$ uncorrected (shown as ± 2.00, i.e., log 10 p values on the scale).

between parietal versus occipital area, we tested whether the ratio between these areas is predicted by linear or quadratic effects of age in our data. No significant age effects were found (Table 4).

The results of our planned analyses showed that occipital lobe area and parietal lobe area make independent and opposite contributions to individual difference in global motion sensitivity and that these effects are not mediated by total cortical surface area. Given this result, we explored more closely how the relationship between

global motion and regional area was distributed over the cortical surface. Local cortical area was regressed point by point across the surface on individual motion thresholds by general linear models, with a smoothed age function, sex, and scanner ID, and (Age × Motion threshold) interaction included as covariates. Figure 3 shows uncorrected maps of the significance of this association. Consistent with the four-lobe analysis, the strongest positive association is seen bilaterally in the parietal lobe, specifically around the IPS and particularly in the supramarginal gyrus on the inferior bank of the sulcus in each hemisphere. The negative association of occipital area with sensitivity to global motion is most apparent around the occipital pole and on the medial surface in the pericalcarine cortex and the cuneus.

Correlations between Global Motion, Global Form, and Cognitive Tests

The finding that global motion performance was associated with increased relative area in the region of the IPS motivated our investigation of its relationship to mathematical and visuomotor skills that have been linked to parietal lobe function. Studentized residuals after controlling for age and sex were calculated for motion and form coherence thresholds and raw scores on the VMI, Woodcock–Johnson Calculation and Applied Problems subtests, and the Panamath test. To compare with a nonnumerical and nonspatial cognitive task, we also examined similar scores on the NIH Toolbox Oral Reading Recognition test. Table 5 presents the pairwise correlations between these measures.

Global form coherence thresholds showed no significant association with any of the cognitive tests. In marked contrast, global motion coherence thresholds show

Table 5. Intercorrelations of Global Form and Motion Thresholds with Cognitive Test Scores

Test	Behavioral Function	Global Form Coherence	Global Motion Coherence	n
Beery VMI	Visuomotor (drawing)	$r = -.12$	$r = -.25$	147
		$p = .16$	$p = .002$***	
Woodcock–Johnson Applied Problems subtest	Mathematics—word problems	$r = -.05$	$r = -.21$	88
		$p = .66$	$p = .05$*	
Woodcock–Johnson Calculation subtest	Mathematics—numerical problems	$r = -.04$	$r = -.17$	144
		$p = .67$	$p = .05$*	
Panamath % correct	Numerosity judgment	$r = -.22$	$r = -.29$	62
		$p = .76$	$p = .02$*	
NIH Toolbox Reading	Reading single words	$r = .02$	$r = .08$	133
		$p = .80$	$p = .35$	

Correlations calculated on studentized residuals of raw test scores against age and sex. Note that low thresholds indicate good performance—hence negative correlations. Results with significance levels of $p \leq .05$ are indicated in bold type (*$p \leq .05$, ***$p \leq .005$).

significant correlations with VMI scores and all the mathematical/numerical scores. Calculation scores show a high correlation with scores on the Toolbox Reading test ($r = .37$, $p < .0001$) but despite this, the latter show no significant relationship to global motion thresholds, indicating that the association with motion is specific to mathematical and spatial cognition rather than to general measures of scholastic attainment. Furthermore, global motion and global form thresholds are highly correlated ($r = .54$, $p < .0001$). Their differing relationships with the other cognitive measures indicate that performance on these latter measures is specifically associated with global motion, rather than with any more general ability to attend to visual stimulus information or detect signals in noise, demands which are common to the global form and motion tasks.

Despite the association between global motion performance and the VMI and numerical cognition tests, none of the latter showed a significant association with area of any of the cortical lobes.

DISCUSSION

Global Motion Processing and Brain Structure

A striking general feature of these results is that the pattern of association for global motion sensitivity, both with children's cortical structure and with their cognitive performance, is specific to that ability and is not shared with global form sensitivity despite the analogous general cognitive demands of the two tasks. Instead, it appears linked, as hypothesized, to processing by the dorsal stream. Specifically, this link appears as an association with a relatively larger surface area of the parietal cortex, most strongly in the lower bank of the IPS, especially the supramarginal gyrus.

Global motion performance was also associated with relatively reduced area of the occipital lobe. The effects of parietal and occipital area make independent contributions to performance, in that they appear in a model where area of each lobe is treated as a regressor. Total cortical area was not separately controlled for in this analysis, so the relation to reduced occipital area does not simply reflect a reduced proportional share due to increased parietal area. However, the results suggest that a particular phenotype of cerebral morphology might be associated with global motion sensitivity. Because global motion sensitivity improves markedly with age, this raises the possibility that this morphological pattern may reflect overall brain maturation. We think that this is unlikely. Although there is a general trend in child development for more growth in the anterior parts of the brain, such data give little indication of differential expansion of parietal and occipital areas (Jernigan, Brown, Bartsch, & Dale, 2016; Brown & Jernigan, 2012), and the contraction of cortical area (which is particularly striking in the occipital lobe) appears only at age 12 and

beyond, that is, after the age range studied here. This is supported by the present sample in which the parietal/occipital area ratio shows no significant variation with age (Table 4).

It is noteworthy that there is no evidence of a positive association of individual differences in motion sensitivity with the extrastriate visual areas known to be involved in global motion processing. These areas form a relatively small fraction of the occipital lobe, and so the negative association with occipital area says little about their role. In any case, the results should not be interpreted as indicating that these areas are irrelevant to motion processing. Rather, they suggest that the source of children's individual variability in motion performance is not in these areas but in parietal areas to which they project in the dorsal stream. Primate neurophysiological experiments (Hanks, Ditterich, & Shadlen, 2006; Shadlen & Newsome, 2001) have shown that signals related to global motion are transmitted from area MT to neurons in the IPS, which accumulate the evidence used in monkeys' psychophysical judgments of motion. Our results are consistent with the possibility that individual differences in performance are dominated by this stage of perceptual decision-making based on evidence accumulation, rather than the earlier level of generating global motion signals.

The absence of similar effects for global form implies that the anatomical differences are specific to motion perception, rather than any general capacity for making decisions on perceptual evidence. There appear to be no analogous studies to Shadlen and Newsome's work that examine neurons integrating global form information. However, several human neuroimaging studies have been used to argue that perceptual decisions based on ventral stream information are made in areas such as inferior temporal cortex (Tremell & Wheeler, 2015; Pins, Meyer, Foucher, Humphreys, & Boucart, 2014) or dorsolateral pFC (Heekeren, Marrett, Bandettini, & Ungerleider, 2004). Thus, the limited evidence available suggests that perceptual decisions are mediated by domain-specific cortical systems rather than by a common structure.

Global Motion Processing, Numerical and Spatial Skills

We hypothesized that global motion performance is associated with the dorsal stream of cortical processing and with cognitive functions that depend on structures in this stream, notably in the parietal cortex. The identified effect of parietal area was strongest in the region of the IPS, especially in the supramarginal gyrus. A number of studies show involvement of this area in numerical cognition. It is activated in adults and children solving novel mathematical problems (Cantlon, Brannon, Carter, & Pelphrey, 2006; Dehaene, Piazza, Pinel, & Cohen, 2003) and in responses to numerosity (Castelli, Glaser, & Butterworth, 2006; Piazza, Izard, Pinel, Le Bihan, & Dehaene, 2004)

even in infants (Izard, Dehaene-Lambertz, & Dehaene, 2008), and it shows differential structural development (Ranpura et al., 2013; Isaacs, Edmonds, Lucas, & Gadian, 2001) and reduced responses in numerical processing (Mussolin et al., 2010; Price, Holloway, Räsänen, Vesterinen, & Ansari, 2007; Kucian et al., 2006) in children with dyscalculia. Consistent with this, our data showed that children's motion sensitivity was associated with performance on tests of numerical cognition, both simple numerosity judgments (Panamath) and tests of mathematical achievement requiring arithmetical manipulations (Woodcock–Johnson). However, as mentioned, these tests did not show a relationship with parietal area, suggesting that a more extended network of cortical structures is required for processing in the mathematical tasks.

Although the Woodcock–Johnson scores were well correlated with word reading, reflecting overall scholastic achievement, reading scores were not correlated with motion sensitivity in our sample, suggesting that the association of motion is not with overall scholastic aptitude or achievement but is a specific relation between cognitive functions that share parietal lobe involvement. The lack of a relationship with the word reading test may be surprising in the light of extensive evidence that global motion performance is impaired in developmental dyslexia (Benassi, Simonelli, Giovagnoli, & Bolzani, 2010, provide an extensive review and meta-analysis). However, we note, first, that differences between dyslexics and typically developing children do not necessarily reflect the correlates of variations in reading skill among the typically developing, who would be the large majority in the present sample. Second, the evidence for the association comes either from fluency in reading continuous text or from very specific tests such as nonword reading (Witton et al., 1998) or the incidence of letter transpositions (Cornelissen, Hansen, Hutton, Evangelinou, & Stein, 1998). All these tests make demands beyond the recognition of single printed words, the basis of the Toolbox test used here.

Another broad function of the parietal lobe is the transformation of visuospatial into motor representations (Culham & Valyear, 2006; Jackson & Husain, 2006). We therefore expected that global motion sensitivity might show a correlation with the visual-spatial-motor skills measured by the VMI test, and this was confirmed. Again, no such relationship was present for global form sensitivity, supporting the hypothesis of a specific dorsal stream system underlying variations in these abilities.

The dissociation between correlates of global form and global motion measures is particularly striking given the relatively high correlation between them: They share 18% of their variance, but this shared variance appears to contribute little to the other cognitive and neuroimaging measures. We suggest that the shared variance reflects specific task requirements for identifying visual structure in noise, but not the broader neurocognitive attributes underlying the relationships of global motion performance to visuomotor integration and calculation. Overall, it is clear that global motion thresholds provide a considerably more sensitive indicator of individual children's neurocognitive development than variations in global form thresholds. This may reflect the fact that global motion sensitivity varies more across age and individuals. However, the correlation between global form and global motion sensitivity demonstrates that both thresholds have substantial and functionally meaningful variation. Furthermore, the correlation between the first and second measurement of global form thresholds ($r = .606$, $p < .0001$) is actually higher than the corresponding figure for global motion thresholds ($r = .471$, $p < .0001$. We conclude that the lack of relationships between global form sensitivity and neurocognitive measures is unlikely simply to reflect a lack of systematic variance in the former.

Our results are consistent with reports that 10-year-olds in high and low ability bands for mathematics differ on motion but not form coherence thresholds (Sigmundsson, Anholt, & Talcott, 2010) and that global motion thresholds at 5 years predict subtraction performance at 8 years (Boets, De Smedt, & Ghesquière, 2011). They may be related to the finding of Anobile, Stievanno, and Burr (2013) that children's performance on numerosity judgments and calculation (but not text reading) is correlated with performance on attention tracking of moving objects (although the latter task makes very different demands on motion processing from detecting global motion coherence). The results are also consistent with the report that TMS over the ventral IPS area impairs both coherent motion performance and the speed of numeral comparison (Salillas, Basso, Baldi, Semenza, & Vecchi, 2009).

Interpretation of Cortical Area Variations

Some cautions are necessary in interpreting the structural findings. First, there is little evidence on what variations in relative cortical expansion may signify in terms of detailed brain structure. We do not know whether a larger area reflects more neurons, greater connectivity, more myelination, increased cell column width, or some other anatomical variation. Future analysis of diffusion weighted data may be able to test the role of neural connectivity in the relationships we have found.

Second, we do not yet know the developmental significance of our cortical area measures. They may reflect genetically based differences in local cortical growth rates, as has been found for age-rated changes in cortical thickness (Fjell, Grydeland, et al., 2015). However, they do not necessarily imply any change in area relationships over age: The basis of the individual differences identified in this study may have been present prenatally (and could include variations in the number of radial

units and neuronal number) or alternatively could reflect differential expansion during development (which more probably would involve differential connectivity). An effect of the latter kind could reflect differential experience: Two-way relationships between behavior and brain structure are possible. The PLING data set will in due course yield longitudinal data that may help to resolve this question.

Conclusion

In conclusion, our findings indicate that global motion performance can provide a specific and sensitive indica-

tor of brain development among typically developing children, whose variation is associated particularly with parietal structure and with individual differences in spatial and numerical cognition. The link to mathematical cognition and visuomotor skill is consistent with a common parietal basis for variation in these functions.

Global motion sensitivity has been established as an indicator of neural systems that are vulnerable in many developmental disorders. The present results extend this idea to variations in typical development and suggest that the IPS and supramarginal gyrus may be key structures in mediating these developmental relationships, as elements in a cerebral phenotype, which also

APPENDIX A
Fuller results of the regression models cited in Tables 2–4 are presented below.

Table A1. Results of Regression Models Predicting Global Motion and Form Thresholds from Bilateral Cortical Surface Areas of Each of the Four Cerebral Lobes (Table 2)

Prediction	Global Motion Threshold		Global Form Threshold	
Term	t Ratio	Prob > |t|	t Ratio	Prob > |t|
Intercept	7.41	<0.0001	3.94	0.0001
Age	−7.99	<0.0001	−3.64	0.0004
Age-squared	4.69	<0.0001	1.83	0.069
Sex	−1.06	0.29	−0.27	0.79
Scanner	−0.91	0.36	−0.10	0.92
Occipital area	2.15	0.033	0.30	0.76
Parietal area	−2.08	0.040	0.43	0.67
Temporal area	−0.55	0.58	0.01	0.99
Frontal area	0.33	0.74	−1.05	0.29

Variables predicting high sensitivity show a negative effect because this corresponds to low threshold.

Table A2. Results of Regression Models Testing Separately the Prediction of Global Motion Thresholds from Bilateral Parietal Area and Bilateral Occipital Area (Table 3)

Prediction	Global Motion Threshold from Parietal Area		Global Motion Threshold from Occipital Area	
Term	t Ratio	Prob > |t|	t Ratio	Prob > |t|
Intercept	8.14	<0.0001	7.63	<0.0001
Age	−8.50	<0.0001	−7.87	<0.0001
Age-squared	4.45	<0.0001	4.01	<0.0001
Sex	−1.06	0.29	−1.13	0.26
Scanner	−1.01	0.31	−0.80	0.43
Total cortical area	1.58	0.12	−3.21	0.0016
Bilateral lobe area	−2.36	0.019	2.42	0.0166
Bilateral lobe area × Age	1.54	0.13	1.30	0.20

Variables predicting high sensitivity show a negative effect because this corresponds to low threshold.

Table A3. Parietal/Occipital Area Ratio Is Independent of Age: Results of Regression Model Testing Prediction of Parietal/ Occipital Ratio from Age and Age-squared (Table 4)

Prediction	Parietal/Occipital Area Ratio from Age	
Term	t Ratio	Prob > |t|
Intercept	48.68	<0.0001
Age	1.18	0.24
Age-squared	0.14	0.89
Sex	−1.21	0.23
Scanner	−1.28	0.20

involves reduced area of the occipital lobe. These brain areas may be critical in the functional effects of many pathologies.

REFERENCES

Akshoomoff, N., Newman, E., Thompson, W. K., McCabe, C., Bloss, C. S., Chang, L., et al. (2014). The NIH Toolbox Cognition Battery: Results from a large normative developmental sample (PING). *Neuropsychology, 28,* 1–10.

Albright, T. D., & Stoner, G. R. (1995). Visual motion perception. *Proceedings of the National Academy of Sciences, U.S.A., 92,* 2433–2440.

Anobile, G., Stievanno, P., & Burr, D. C. (2013). Visual sustained attention and numerosity sensitivity correlate with math achievement in children. *Journal of Experimental Child Psychology, 116,* 380–391.

Atkinson, J., & Braddick, O. (2005). Dorsal stream vulnerability and autistic disorders: The importance of comparative studies of form and motion coherence in typically developing children and children with developmental disorders. *Cahiers de Psychologie Cognitive/Current Psychology of Cognition, 23,* 49–58.

Atkinson, J., & Braddick, O. (2007). Visual and visuocognitive development in children born very prematurely. *Progress in Brain Research, 164,* 123–149.

Atkinson, J., & Braddick, O. (2011). From genes to brain development to phenotypic behavior: "Dorsal-stream vulnerability" in relation to spatial cognition, attention, and planning of actions in Williams syndrome (WS) and other developmental disorders. *Progress in Brain Research, 189,* 261–283.

Atkinson, J., & Braddick, O. (2012). Visual attention in the first years: Typical development and developmental

disorders. *Developmental Medicine & Child Neurology, 54,* 589–595.

Bartsch, H., Thompson, W. K., Jernigan, T. L., & Dale, A. M. (2014). A web-portal for interactive data exploration, visualization, and hypothesis testing. *Frontiers in Neuroinformatics, 8,* 25.

Beery, K. E. (Ed.) (1989). *Developmental test of visual motor integration: Administration, scoring and teaching manual* (3rd ed., Rev. ed.). Cleveland, OH: Modern Curriculum Press.

Benassi, M., Simonelli, L., Giovagnoli, S., & Bolzani, R. (2010). Coherence motion perception in developmental dyslexia: A meta-analysis of behavioral studies. *Dyslexia, 16,* 341–357.

Biagi, L., Crespi, S. A., Tosetti, M., & Morrone, M. C. (2015). BOLD response selective to flow-motion in very young infants. *PLoS Biology, 13,* e1002260.

Boets, B., De Smedt, B., & Ghesquière, P. (2011). Coherent motion sensitivity predicts individual differences in subtraction. *Research in Developmental Disabilities, 32,* 1075–1080.

Braddick, O., & Atkinson, J. (2011). Development of human visual function. *Vision Research, 51,* 1588–1609.

Braddick, O., Atkinson, J., & Wattam-Bell, J. (2003). Normal and anomalous development of visual motion processing: Motion coherence and "dorsal stream vulnerability". *Neuropsychologia, 41,* 1769–1784.

Braddick, O. J., O'Brien, J. M. D., Wattam-Bell, J., Atkinson, J., & Turner, R. (2000). Form and motion coherence activate independent, but not dorsal/ventral segregated, networks in the human brain. *Current Biology, 10,* 731–734.

Braddick, O. J., O'Brien, J. M. D., Wattam-Bell, J., Atkinson, J., & Turner, R. (2001). Brain areas sensitive to coherent visual motion. *Perception, 30,* 61–72.

Britten, K. H., Shadlen, M. N., Newsome, W. T., & Movshon, J. A. (1992). The analysis of visual motion: A comparison of neuronal and psychophysical performance. *Journal of Neuroscience, 12,* 4745–4765.

Brown, T. T., & Jernigan, T. L. (2012). Brain development during the preschool years. *Neuropsychological Review, 22,* 313–333.

Brown, T. T., Kuperman, J. M., Chung, Y., Erhart, M., McCabe, C., Hagler, D. J., et al. (2012). Neuroanatomical assessment of biological maturity. *Current Biology, 22,* 1693–1698.

Butterworth, B., & Walsh, V. (2011). Neural basis of mathematical cognition. *Current Biology, 21,* R618–R621.

Cantlon, J. F., Brannon, E. M., Carter, E. J., & Pelphrey, K. A. (2006). Functional imaging of numerical processing in adults and 4-year-old children. *PLoS Biology, 4,* e125.

Castelli, F., Glaser, D. E., & Butterworth, B. (2006). Discrete and analogue quantity processing in the parietal lobe: A functional MRI study. *Proceedings of the National Academy of Sciences, U.S.A., 103,* 4693–4698.

Chen, C.-H., Gutierrez, E. D., Thompson, W., Panizzon, M. S., Jernigan, T. L., Eyler, L. T., et al. (2012). Hierarchical genetic organization of human cortical surface area. *Science, 335,* 1634–1636.

Cornelissen, P. L., Hansen, P. C., Hutton, J. L., Evangelinou, V., & Stein, J. F. (1998). Magnocellular visual function and children's single word reading. *Vision Research, 38,* 471–482.

Culham, J. C., & Valyear, K. F. (2006). Human parietal cortex in action. *Current Opinion in Neurobiology, 16,* 205–212.

Dale, A. M., Fischl, B., & Sereno, M. I. (1999). Cortical surface-based analysis. I. Segmentation and surface reconstruction. *Neuroimage, 9,* 179–194.

Dehaene, S., Piazza, M., Pinel, P., & Cohen, L. (2003). Three parietal circuits for number processing. *Cognitive Neuropsychology, 20,* 487–506.

Fischl, B., Salat, D. H., van der Kouwe, A. J., Makris, N., Ségonne, F., Quinn, B. T., et al. (2004). Sequence-independent

segmentation of magnetic resonance images. *Neuroimage, 23(Suppl. 1),* S69–S84.

Fischl, B., Sereno, M. I., & Dale, A. M. (1999). Cortical surface-based analysis. II: Inflation, flattening, and a surface-based coordinate system. *Neuroimage, 9,* 195–207.

Fischl, B., van der Kouwe, A., Destrieux, C., Halgren, E., Ségonne, F., Salat, D. H., et al. (2004). Automatically parcellating the human cerebral cortex. *Cerebral Cortex, 14,* 11–22.

Fjell, A. M., Grydeland, H., Krogsrud, S. K., Amlien, I., Rohani, D. A., Ferschmann, L., et al. (2015). Development and aging of cortical thickness correspond to genetic organization patterns. *Proceedings of the National Academy of Sciences, U.S.A., 112,* 15462–15467.

Fjell, A. M., Walhovd, K. B., Brown, T. T., Kuperman, J. M., Chung, Y., Hagler, D. J., Jr., et al. (2012). Multimodal imaging of the self-regulating developing brain. *Proceedings of the National Academy of Sciences, U.S.A., 109,* 19620–19625.

Fjell, A. M., Westlye, L. T., Amlien, I., Tamnes, C. K., Grydeland, H., Engvig, A., et al. (2015). High-expanding cortical regions in human development and evolution are related to higher intellectual abilities. *Cerebral Cortex, 25,* 26–34.

Gallant, J. L., Braun, J., & Van Essen, D. C. (1993). Selectivity for polar, hyperbolic, and Cartesian gratings in macaque visual cortex. *Science, 259,* 100–103.

Gershon, R. C., Cella, D., Fox, N. A., Havlik, R. J., Hendrie, H. C., & Wagster, M. V. (2010). Assessment of neurological and behavioural function: The NIH Toolbox. *Lancet Neurology, 9,* 138–139.

Gunn, A., Cory, E., Atkinson, J., Braddick, O., Wattam-Bell, J., Guzzetta, A., et al. (2002). Dorsal and ventral stream sensitivity in normal development and hemiplegia. *NeuroReport, 13,* 843–847.

Halberda, J., & Feigenson, L. (2008). Developmental change in the acuity of the "number sense": The approximate number system in 3-, 4-, 5-, and 6-year-olds and adults. *Developmental Psychology, 44,* 1457–1465.

Hanks, T. D., Ditterich, J., & Shadlen, M. N. (2006). Microstimulation of macaque area LIP affects decision-making in a motion discrimination task. *Nature Neuroscience, 9,* 682–689.

Heekeren, H. R., Marrett, S., Bandettini, P. A., & Ungerleider, L. G. (2004). A general mechanism for perceptual decision-making in the human brain. *Nature, 431,* 859–862.

Helfrich, R. F., Becker, H. G., & Haarmeier, T. (2013). Processing of coherent visual motion in topographically organized visual areas in human cerebral cortex. *Brain Topography, 26,* 247–263.

Holloway, I. D., & Ansari, D. (2010). Developmental specialization in the right intraparietal sulcus for the abstract representation of numerical magnitude. *Journal of Cognitive Neuroscience, 22,* 2627–2637.

Inglis, M., & Gilmore, C. (2014). Indexing the approximate number system. *Acta Psychologica, 145,* 147–155.

Isaacs, E. B., Edmonds, C. J., Lucas, A., & Gadian, D. G. (2001). Calculation difficulties in children of very low birthweight: A neural correlate. *Brain, 124,* 1701–1707.

Izard, V., Dehaene-Lambertz, G., & Dehaene, S. (2008). Distinct cerebral pathways for object identity and number in human infants. *PLoS Biology, 6,* e11.

Jackson, S. R., & Husain, M. (2006). Visuomotor functions of the posterior parietal cortex. *Neuropsychologia, 44,* 2589–2593.

Jernigan, T. L., Brown, T. T., Bartsch, H., & Dale, A. M. (2016). Toward an integrative science of the developing human mind and brain: Focus on the developing cortex. *Developmental Cognitive Neuroscience, 18,* 2–11.

Jernigan, T. L., Brown, T. T., Hagler, D. J., Jr., Akshoomoff, N., Bartsch, H., Newman, E., et al. (2016). The pediatric imaging, neurocognition, and genetics (PING) data repository. *Neuroimage, 124,* 1149–1154.

Kontsevich, L. L., & Tyler, C. W. (1999). Bayesian adaptive estimation of psychometric slope and threshold. *Vision Research, 39,* 2729–2737.

Kravitz, D. J., Saleem, K. S., Baker, C. I., & Mishkin, M. (2011). A new neural framework for visuospatial processing. *Nature Reviews Neuroscience, 12,* 217–230.

Kucian, K., Loenneker, T., Dietrich, T., Dosch, M., Martin, E., & von Aster, M. (2006). Impaired neural networks for approximate calculation in dyscalculic children: A functional MRI study. *Behavioral & Brain Functions, 2,* 31.

Lyall, A. E., Shi, F., Geng, X., Woolson, S., Li, G., Wang, L., et al. (2015). Dynamic development of regional cortical thickness and surface area in early childhood. *Cerebral Cortex, 25,* 2204–2212.

Menon, V. (2010). Developmental cognitive neuroscience of arithmetic: Implications for learning and education. *ZDM, 42,* 515–525.

Milner, A. D., & Goodale, M. A. (1995). *The visual brain in action.* Oxford: Oxford University Press.

Mishkin, M., Ungerleider, L., & Macko, K. A. (1983). Object vision and spatial vision: Two critical pathways. *Trends in Neurosciences, 6,* 414–417.

Mussolin, C., De Volder, A., Grandin, C., Schlögel, X., Nassogne, M. C., & Noël, M. P. (2010). Neural correlates of symbolic number comparison in developmental dyscalculia. *Journal of Cognitive Neuroscience, 22,* 860–874.

Newman, E., Thompson, W. K., Bartsch, H., Hagler, D. J., Jr., Chen, C. H., Brown, T. T., et al. (2016). Anxiety is related to indices of cortical maturation in typically developing children and adolescents. *Brain Structure & Function, 221,* 3013–3025.

Newsome, W. T., & Paré, E. B. (1988). A selective impairment of motion perception following lesions of the middle temporal visual area (MT). *Journal of Neuroscience, 8,* 2201–2211.

Nieder, A., & Dehaene, S. (2009). Representation of number in the brain. *Annual Review of Neuroscience, 32,* 185–208.

Orban, G. A., Fize, D., Peuskens, H., Denys, K., Nelissen, K., Sunaert, S., et al. (2003). Similarities and differences in motion processing between the human and macaque brain: Evidence from fMRI. *Neuropsychologia, 41,* 1757–1768.

Piazza, M., Izard, V., Pinel, P., Le Bihan, D., & Dehaene, S. (2004). Tuning curves for approximate numerosity in the human intraparietal sulcus. *Neuron, 44,* 547–555.

Pins, D., Meyer, M. E., Foucher, J., Humphreys, G., & Boucart, M. (2014). Neural correlates of implicit object identification. *Neuropsychologia, 42,* 1247–1259.

Pitzalis, S., Sereno, M. I., Committeri, G., Fattori, P., Galati, G., Patria, F., et al. (2010). Human V6: The medial motion area. *Cerebral Cortex, 20,* 411–424.

Price, G. R., Holloway, I., Räsänen, P., Vesterinen, M., & Ansari, D. (2007). Impaired parietal magnitude processing in developmental dyscalculia. *Current Biology, 17,* R1042–R1043.

Ranpura, A., Isaacs, E., Edmonds, E., Singhal, M. A., Clayden, J., Clark, C., et al. (2013). Developmental trajectories of grey and white matter in dyscalculia. *Trends in Neuroscience & Education, 2,* 56–64.

Raznahan, A., Shaw, P., Lalonde, F., Stockman, M., Wallace, G. L., Greenstein, D., et al. (2011). How does your cortex grow? *Journal of Neuroscience, 31,* 7174–7177.

Salillas, E., Basso, D., Baldi, M., Semenza, C., & Vecchi, T. (2009). Motion on numbers: Transcranial magnetic stimulation on the ventral intraparietal sulcus alters both numerical and motion processes. *Journal of Cognitive Neuroscience, 21,* 2129–2138.

Shadlen, M. N., & Newsome, W. T. (2001). Neural basis of a perceptual decision in the parietal cortex (area LIP.)

of the rhesus monkey. *Journal of Neurophysiology, 86,* 1916–1936.

Sigmundsson, H., Anholt, S. K., & Talcott, J. B. (2010). Are poor mathematics skills associated with visual deficits in temporal processing? *Neuroscience Letters, 469,* 248–250.

Sunaert, S., Van Hecke, P., Marchal, G., & Orban, G. A. (1999). Motion responsive regions of the human brain. *Experimental Brain Research, 127,* 355–370.

Tremell, J. J., & Wheeler, M. E. (2015). Content-specific evidence accumulation in inferior temporal cortex during perceptual decision-making. *Neuroimage, 109,* 35–49.

Tudusciuc, O., & Nieder, A. (2007). Neuronal population coding of continuous and discrete quantity in the primate posterior parietal cortex. *Proceedings of the National Academy of Sciences, U.S.A., 104,* 14513–14518.

Wattam-Bell, J. (1994). Coherence thresholds for discrimination of motion direction in infants. *Vision Research, 34,* 877–883.

Wattam-Bell, J., Birtles, D., Nyström, P., von Hofsten, C., Rosander, K., Anker, S., et al. (2010). Reorganization of global form and motion processing during human visual development. *Current Biology, 20,* 411–415.

Witton, C., Talcott, J., Hansen, P., Richardson, P., Griffiths, T., Rees, A., et al. (1998). Sensitivity to dynamic auditory and visual stimuli predicts nonword reading ability in both dyslexic and normal readers. *Current Biology, 8,* 791–797.

Woodcock, R. W., McGrew, K. S., & Mather, N. (2001). *Woodcock–Johnson III.* Itasca, IL: Riverside Publishing.